Accepted Manuscript

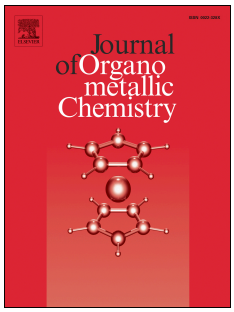

Aminoacid-derivatized Cu (II) complexes: Synthesis, DNA interactions and *in vitro* cytotoxicity

Rinky Singh, P. Rama Devi, Sharmita S. Jana, Ranjitsinh V. Devkar, Debjani Chakraborty

PII: S0022-328X(17)30245-0

DOI: 10.1016/j.jorganchem.2017.04.017

Reference: JOM 19904

To appear in: *Journal of Organometallic Chemistry*

Received Date: 23 January 2017

Revised Date: 10 April 2017

Accepted Date: 15 April 2017

Please cite this article as: R. Singh, P.R. Devi, S.S. Jana, R.V. Devkar, D. Chakraborty, Aminoacid-derivatized Cu (II) complexes: Synthesis, DNA interactions and *in vitro* cytotoxicity, *Journal of Organometallic Chemistry* (2017), doi: 10.1016/j.jorganchem.2017.04.017.

Aminoacid-derivatized Cu (II) complexes: Synthesis, DNA interactions and *in vitro* Cytotoxicity.

Rinky Singh [a] , Sharmita S Jana[b] , P. Rama Devi [a], Ranjitsinh V Devkar[b], Debjani Chakraborty[a]*

[a]*Department of Chemistry, Faculty of Science, The M .S .University of Baroda, Vadodara-390002, Gujarat, India.*

[b]*Division of Phytotherapeutics and Metabolic Endocrinology, Faculty of Science, The M .S .University of Baroda, Vadodara-390002, Gujarat, India.*

Email id: *debchak23@gmail.com .Tel: +91-9537521703*

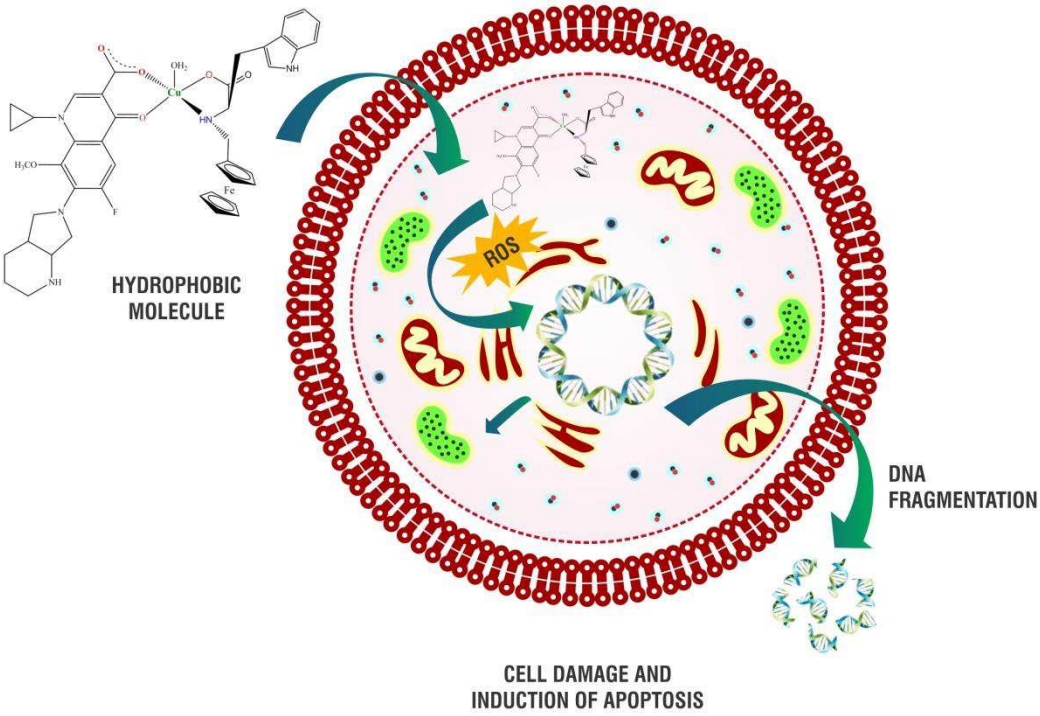

Aminoacid-derivatized Cu (II) complexes: Synthesis, DNA interactions and *in vitro* Cytotoxicity.

Rinky Singh [a] , P. Rama Devi [a], Sharmita S Jana[b], Ranjitsinh V Devkar [b], Debjani Chakraborty[a]*

[a]*Department of Chemistry, Faculty of Science, The M .S .University of Baroda, Vadodara-390002, Gujarat, India.*
[b]*Division of Phytotherapeutics and Metabolic Endocrinology, Department of Zoology, Faculty of Science, The M .S .University of Baroda, Vadodara-390002, Gujarat, India.*
Email id: *debchak23@gmail.com .Tel: +91-9537521703*

Abstract

Two different series of copper complexes, **[Cu(MFL)(FcAA)H_2O] (C1-C4) and [Cu(MFL)(BzAA)H_2O] (C5-C8),** where FcAA= ferrocenyl amino acid mannich base conjugates and BzAA = benzaldehyde amino acid mannich base conjugates have been synthesized and characterized by spectroscopic methods. The complexes have been investigated for their interactions with DNA by employing fluorescence quenching measurements, UV–Vis spectroscopy and DNA viscosity measurements. High binding constants obtained from the DNA binding studies (K_b= 10^6 M^{-1}) prompted the in-vitro cytotoxicity assay of complexes on A549 human lung carcinoma cells (employing MTT assay). The IC_{50} values obtained herein were found to be lower than those of the ligands for A549 cell line. Antiproliferative effects on A549 tumour cells exerted by the complexes were consistent with their intracellular uptake properties. The cellular uptake studies indicated that complexes **C1-C8** enter the cytoplasm and accumulate in the nuclei. Rapid change in the nuclear morphology was observed with DAPI staining. Acridine orange/ethidium bromide dual staining revealed that most of the A549 cells enter early apoptosis within 12 h of treatment. Further all the complexes showed effective cell growth inhibition by triggering G0/G1 phase arrest and inducing apoptosis. FACScan results revealed remarkably high percentage of cell death induced by the complexes in the A549 cells, as compared to control. Annexin-V/PI staining of cells also indicated that the complexes induce cell death through the apoptotic pathway. Our data here suggests that the complexes could be good antitumor agents.

Key words: Copper complexes, ferrocenyl mannich bases, DNA Binding, DNA Cleavage, A549 cells, Apoptosis.

1. Introduction

Medicinal inorganic chemistry offers additional opportunities for the design of therapeutic agents not accessible to organic compounds [1−3].The wide range of coordination numbers and geometries, available redox states, thermodynamic and kinetic characteristic, and intrinsic properties of the cationic metal ion and ligand itself offer the medicinal chemist a large variety of reactivity to be exploited. The widespread success of cisplatin in the clinical treatment of various types of neoplasia has placed coordination chemistry of metal-based drugs in frontline in the fight against cancer [1, 4]. Although highly effective in treating a variety of cancers, the cure with cisplatin is still limited by dose-limiting side effects [5] and inherited or acquired resistance phenomena, only partially amended by employment of new platinum drugs [6−9]. These problems have stimulated an extensive search and prompted chemists to develop alternative strategies, based on different metals, with improved pharmacological properties and aimed at different targets [10].

The ferrocene derivatives among the metallocenes are of importance for their stability in a biological medium and for their lipophilic, nontoxic, and reversible redox properties [11]. The cyclopentadienyl rings of ferrocene could be suitably functionalized, and ferrocenyl derivatives are known to exhibit antitumor, antimalarial, and antifungal properties [11]. Seio *et al*. [12] have reported new DNA binding molecules utilizing structural and conformational properties of ferrocene. Their design concept is based on the fact that the distance between the two cyclopentadienyl rings of ferrocene, ca. 3.3 Å is close to the distance between two aromatic rings stacked with each other. In addition, it is well-known that the minor groove of DNA can accommodate stacked aromatic rings, as established by the structural studies of natural or synthetic molecules that recognize the minor groove. Studies on the binding of ferrocenyl ligands with DNA has revealed binding constants in the order of 10^3-10^5 M^{-1} [13] thus agreeing with the above mentioned fact. The stability of ferrocene in aqueous and aerobic media has made ferrocenyl compounds very popular molecules for such biological applications. Furthermore such favourable characteristics of ferrocene led to the design of ferrocenyl derivatives that function as highly sensitive detectors of proteins or as reporters of protein activity. Studies on ferrocenyl conjugates with amino acids and end-labelled ferrocenyl di- and tripeptides have demonstrated distinctive electrical, structural, and medicinal properties [14]. Many researchers have shown interest in design of unnatural ferrocenyl amino acids and peptides which further have been studied for their biomedical applications.

Modification of proteins by incorporating such unnatural ferrocenyl amino acids helps the study of protein structure, activity and interaction with other biomolecules [15].

The ferrocenyl compounds are known to hold good potential as anticancer agents. This can be exemplified by the fact that ferrocifen, the ferrocene-appended anticancer drug tamoxifen, makes the drug effective against both hormone-independent and hormone-dependent breast cancer cells [16]. Similarly, ferroquine, the ferrocene-attached antimalarial drug chloroquine, has been found to be more effective than chloroquine [17]. The ability of ferrocenyl compounds to cleave DNA may be responsible for these diverse properties [18–20]. Recent reports from our laboratory have shown that Ru (II) complexes of amino acid conjugated ferrocene mannich bases are efficient DNA and serum protein binders. Further, *in-vitro* investigations on A549 and MCF7 cell lines revealed their cytotoxicity and preference for apoptosis [21, 22].

Copper-based complexes have been investigated on the assumption that endogenous metals may be less toxic for normal cells with respect to cancer cells. The altered metabolism of cancer cells and differential response between normal and tumour cells to copper are the basis for development of copper complexes endowed with antineoplastic characteristics. Copper is an essential element for most aerobic organisms, employed as a structural and catalytic cofactor, and consequently it is involved in many biological pathways [23-25]. Taking this into account, much attention has been given to research on the mechanisms of absorption [26], distribution, [27] metabolism, and excretion of copper [28, 29], as well as on its role in development of cancer and other diseases [30, 31]. The fundamental aspects of the chemistry and biochemistry of copper [32], the role of this metal in medicine and the pathology and treatment of Menkes and Wilson diseases [33], and the chelation therapy approach in neurodegenerative disorders characterized by accumulation of abnormal protein components mediated by copper [34] have extensively been surveyed in recent review articles to which readers are addressed for a comprehensive knowledge of the multifaceted functions played by this metal ion in physiology.

Comparing the extensive literature regarding the use of existing clinical drugs and development of novel chemical entities based on platinum, the field of anticancer copper complexes seems only at an infancy stage, even though it shows much promise for future development. Actually, copper complexes offer the potential over platinum (II) complexes of reduced toxicity, a novel mechanism of action, a different spectrum of activity, and the prospect of non-cross-resistance. A recent review by Carlo Santini throws light on the various advances in copper complexes as anticancer agents [35].

Moxifloxacin (MFL) is a 4thgeneration fluroquinolone drug with a broad spectrum of antibacterial properties and thus is an important option in the treatment of bacterial infections [36]. During the past years, the antitumoral activity of MFL has raised much attention. In vitro and in vivo studies have confirmed its anticancer effects to be associated with the inhibition of mammalian DNA topoisomerase I, topoisomerase II, and DNA polymerase. Copper complex of MFL has been found to bind CT-DNA via the intercalative mode and induce apoptosis in A-549 lung cancer cells by DNA damage [37, 38].

The foregoing facts stimulated our interest on the syntheses, structure, DNA binding, cleavage and anticancer properties of mixed ligand Cu(II) complexes of amino acid conjugated ferrocenyl / benzaldehyde mannich bases and the fluoroquinolone antibiotic moxifloxacin. These ferrocenyl amino acids have been targeted as it has been shown that tethering biologically active groups to ferrocenyl unit increases their potency possibly due to combined action of the organic molecule with fenton chemistry of the Fe-centre [39]. The structures of the new complexes were established on the basis of spectroscopic and electrochemical data. In addition, DNA cleavage abilities and anticancer activities of the complexes have been rationalized in terms of their DNA binding affinity. All the complexes show strong binding affinity to DNA, induce apoptosis and act as a good antitumor agent in a dose & time dependent manner.

2. Experimental

2.1. Reagents and Materials

All the chemicals and solvents used for synthesis and characterization of ligands and complexes are of analytical grade and were used as purchased. Ferrocene carboxaldehyde and DAPI stain were purchased from Sigma–Aldrich. Amino acids, CT-DNA, Tri–sodium citrate and EB (ethidium bromide) were purchased from SRL (Sisco Research Laboratory, Mumbai, India). Cu (acetate) $_2$. $2H_2O$ and BSA (bovine serum albumin) were purchased from Hi media. All the solvents used in the present studies were purchased from Merck and are of analytical grade. Moxifloxacin (MFL) was kindly donated by Alembic Research Centre (Gujarat, India).

2.2. Methods and instrumentation

Infrared (IR) spectra (400–4000 cm^{-1}) were recorded on Perkin Elmer RX-1 FTIR with samples prepared as KBr disks. ESI Mass spectra of the ligands were recorded on Thermoscientific DSQ – II Mass spectrometer and those of the complexes were recorded on Applied Biosystem API

2000 Mass spectrometer. C, H and N elemental analysis were performed on a Perkin-Elmer 240B elemental analyser. UV–visible spectra were recorded in solution at concentrations in the range 10^{-5}–10^{-3} M on Perkin Elmer Lambda-35 dual beam UV-Vis spectrophotometer. Fluorescence spectra were recorded in solution on JASCO FP-6300 fluorescence spectrophotometer. EPR spectra at liquid nitrogen temperature were recorded on X-band EPR spectrometer (IIT Mumbai). Fluorescence spectra were recorded in solution on JASCO FP-6300 fluorescence spectrophotometer. The % metal content in each of the complexes was determined by complexometric/gravimetric titration method after decomposition of the complexes. Thermogravimetric analyses were carried out with a model EXSTAR 6000. Cyclic voltammetric studies were performed on CHI-600C electrochemical analyser in a three-electrode system comprising of a glassy carbon working, platinum wire auxiliary, and saturated calomel reference (SCE) electrode. Tetrabutylammonium perchlorate (TBAP) (0.1 M) was used as a supporting Electrolyte in DMSO. Electrochemical data were uncorrected for junction potentials.

2.3. Synthesis of ligands

2.3.1. Synthesis of **L1-L4**

The ferrocenyl amino acids **L1-L4** were synthesised according to the reported procedure [21]. The amino acids (5.0 mmol) and NaOH (5.0 mmol) in dry methanol (10 mL) were stirred for 30 min to get a homogeneous solution. A methanolic solution (10 mL) of ferrocene carboxaldehyde (5.0 mmol) was added dropwise to the above solution, which was refluxed for 90 min, cooled, and treated with sodium borohydride (10.0 mmol) with constant stirring. The solvent was evaporated, the resulting mass was dissolved in water and acidified with dilute HCl, and the solution pH was maintained at 5.6. The ligands precipitated as yellow solids were filtered, thoroughly washed with water and cold methanol, and finally dried in vacuum over P_4O_{10}.

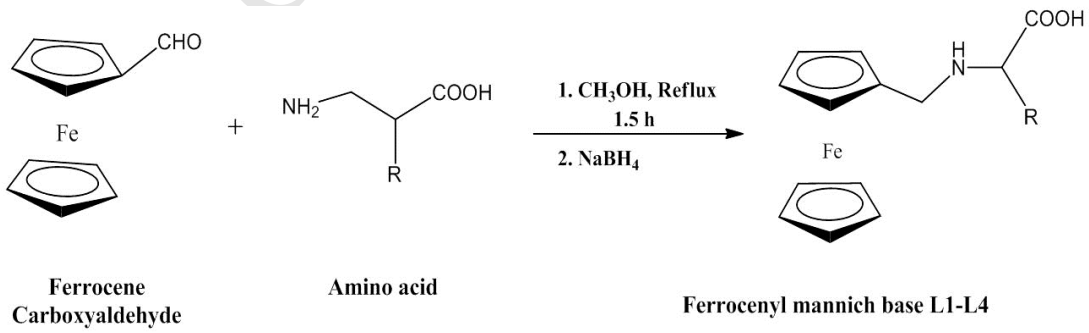

Ferrocene Carboxyaldehyde **Amino acid** **Ferrocenyl mannich base L1-L4**

-R	Amino acid	Ligand	Complex
CH_2(3-indoyl)	Tryptophan	L1	C1
$-CH_2Ph$	Phenyl alanine	L2	C2
$-CH_2CH(CH_3)_2$	Leucine	L3	C3
$-CH_2$(4-hydroxyphenyl)	Tyrosine	L4	C4

SCHEME 1

2.3.2 Synthesis of **L5-L8**

The amino acids (2.0 mmol) were initially dissolved in dry methanol (20 mL) with addition of NaOH (2.0 mmol) and continuous stirring. Benzaldehyde (2.0 mmol) was subsequently added to the above solution. The mixture was refluxed for 1 h, cooled, and then treated with an excess of solid $NaBH_4$ with constant stirring. After stirring for~15 min, the solvent was removed on rotary evaporator and the resulting mass was dissolved in water followed by treatment with dilute HCl to maintain a pH of~5.5. White solids thus precipitated were filtered off, thoroughly washed with water and cold methanol, and finally dried in vacuum over P_4O_{10}.

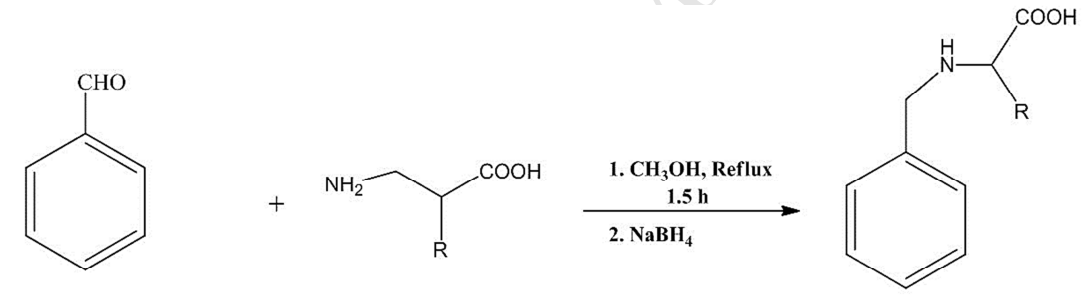

Benzaldehyde **Amino acid** **Mannich base L5-L8**

-R	Amino acid	Ligand	Complex
CH_2(3-indoyl)	Tryptophan	L5	C5
$-CH_2Ph$	Phenyl alanine	L6	C6
$-CH_2CH(CH_3)_2$	Leucine	L7	C7
$-CH_2$(4-hydroxyphenyl)	Tyrosine	L8	C8

SCHEME 2

2.3.3 Synthesis of complexes **C1-C8**

Complexes C**1-C8** were prepared by a general synthetic procedure in which 1.0 mmol of copper(II) acetate in 15 mL of methanol was reacted with moxifloxacin (MFL, 1.0 mmol) in methanol while stirring at room temperature for 0.5 h followed by addition of solid fFc-AA/Bz-AA (1.0 mmol) ligands in small portions with continuous stirring. The reaction mixture was further stirred for 2 h, and the product was isolated as a green solid in~75% yield. The solid was washed with water and cold methanol, and finally dried in vacuum over P_4O_{10} (scheme 1&2).

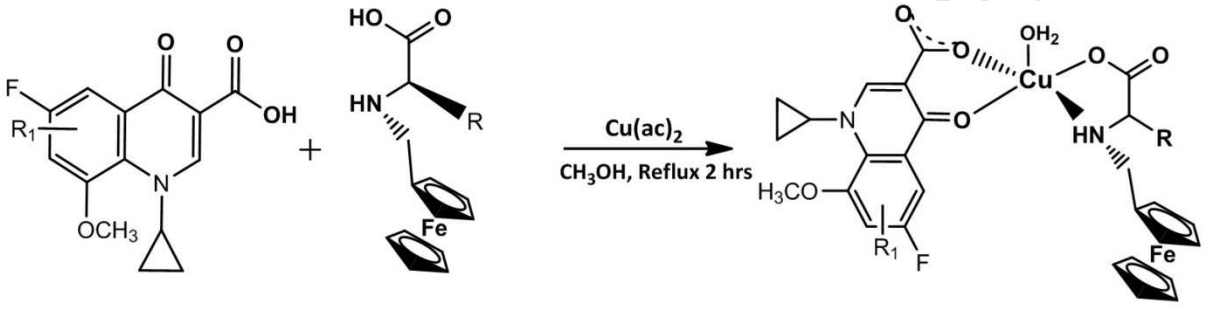

Moxifloxacin **Mannich Base L1-L4** **Cu-Complex C1-C4**

-R	Amino acid	Ligand	Complex
CH_2(3-indoyl)	Tryptophan	L1	C1
-CH_2Ph	Phenyl alanine	L2	C2
-$CH_2CH(CH_3)_2$	Leucine	L3	C3
-CH_2(4-hydroxyphenyl)	Tyrosine	L4	C4

SCHEME 3

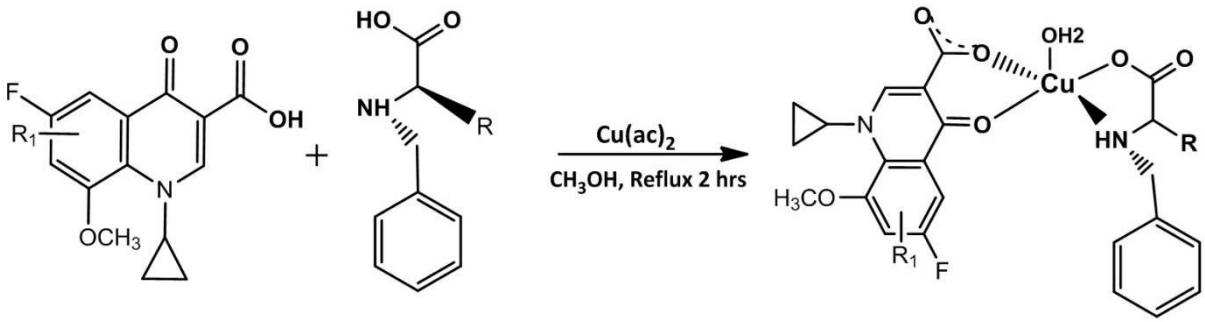

Moxifloxacin **Mannich Base L5-L8** **Cu-Complex C5-C8**

-R	Amino acid	Ligand	Complex
CH_2(3-indoyl)	Tryptophan	L5	C5
$-CH_2Ph$	Phenyl alanine	L6	C6
$-CH_2CH(CH_3)_2$	Leucine	L7	C7
$-CH_2$(4-hydroxyphenyl)	Tyrosine	L8	C8

SCHEME 4

Physicochemical data of the synthesized ligands and complexes have been provided supplementary material.

2.4 DNA binding experiments

2.4.1. UV absorption studies

The interaction of compounds with CT DNA has been studied with UV spectroscopy in order to investigate the possible binding modes to CT DNA and to calculate the binding constants (K_b). Absorption studies were performed with fixed compound concentrations while varying the CT-DNA concentration within. While measuring the absorption, equal increments of CT-DNA were added at different ratios to both the compound solution and the reference solution to eliminate the absorbance of CT-DNA itself.

2.4.2. Competitive binding studies with EB using fluorescence spectroscopy

The competitive binding study of each compound with EB has been investigated with fluorescence spectroscopy in order to examine whether the compound can displace EB from DNA–EB complex. The DNA–EB complex was prepared by adding 2.6 μM EB and 2.0

μM DNA in tris buffer. The binding mode of complexes **C1–C8** with CT-DNA was studied by adding a certain amount of a solution of each complex step by step into the solution of the DNA–EB complex. The influence of the addition of each complex has been obtained by recording the variation in the fluorescence emission spectra of the DNA–EB complex. The fluorescence intensities of EB bound to CT-DNA were measured at 609 nm (524 nm excitation) after addition of different concentrations of the complexes at different ratios.

2.4.3. Competitive binding studies with DAPI using fluorescence spectroscopy

The competitive binding study of **C1–C8** with known groove binder DAPI has been investigated with fluorescence spectroscopy. The DNA–DAPI complex was prepared by adding DAPI (5 μM) and DNA (20 μM) in tris buffer. The binding mode of complexes **C1–C8** with CT-DNA was studied by adding a certain amount of a solution of each complex step by step into the solution of the DNA–DAPI complex. The influence of the addition of each complex has been obtained by recording the variation in the fluorescence emission spectra of the DNA–DAPI complex. The fluorescence intensities of DAPI bound to CT-DNA were measured at 451 nm (340 nm excitation) after addition of different concentrations of the complexes at different mixing (r) ratios.

2.4.4. Viscosity measurements

Cannon–Ubbelohde viscometer maintained at a constant temperature of 32.0 ± 0.1 °C in a thermostat was used to measure the relative viscosity of DNA (200 μM) solutions in the presence of complexes **C1–C8** (with [complex]/[DNA] ratio of 0, 0.04, 0.08, 0.12, 0.16, 0.20 and 0.24) in Tris–HCl buffer (pH 7.2). Digital stopwatch with least count of 0.01 s. was used for flow time measurement with accuracy of ±0.1 s. The flow time of each sample was measured three times and an average flow time was calculated. Data are presented as $(\eta/\eta_0)^{1/3}$ versus [complex]/[DNA], where h is the viscosity of DNA in the presence of complex and h0 is the viscosity of DNA alone. Viscosity values were calculated from the observed flow time of DNA-containing solutions (t) corrected for that of the buffer alone (t_0), $\eta = (t - t_0)/t_0$.

2.5. Nuclease activity

The solution containing metal complex was taken in a clean Eppendorf tube and 1μg of plasmid pBR322 DNA was added. The contents were incubated for 30 minutes at 37 °C and loaded on

0.8% agarose gel after mixing 3µl of loading buffer and 0.25% bromophenol blue + 0.25% Xylene cynaol +30% glycerol. Electrophoresis was performed at constant voltage till the bromophenol blue reached to the 3/4 of the gel. The gel was stained for 10 min by immersing it in ethidium bromide solution (5 µg/ml) and then de-stained for 10 min by keeping it in sterile distilled water. The plasmid bands were visualized by photographing the gel under a UV Trans illuminator. The efficiency of DNA cleavage was measured by determining the ability of the complex to form open circular (OC) or nicked circular (NC) DNA from its super coiled.

2.6. Cytotoxicity

A549 cells ($5.0X10^3$ cells $well^{-1}$) were placed in 96-well culture plates (Tarson India Pvt., Ltd.) and grown overnight at 37°C in a 5% CO_2 incubator. Compounds to be tested were then added to the wells to achieve final concentrations ranging from 10 to 500 mg/ml. Control wells were prepared by addition of culture medium without the compounds. The plates were incubated at 37°C at 5% CO_2 incubator for 24 h. Upon completion of the incubation, MTT dye solution (prepared using serum free culture medium) was added to each well to a final concentration of 0.5 mg/ml. After 4 h of incubation with MTT, the culture media was discarded and the wells were washed with Phosphate Buffer Saline (Hi-Media, India Pvt., Ltd.), followed by addition of DMSO to dissolve the formazan crystals so formed and subsequent incubation for 30 min. The optical density of each well was measured spectrophotometrically at 563 nm using Biotek-ELX800MS universal ELISA reader (Bio-Tek instruments, Inc., Winooski, VT). The IC_{50} values were determined by plotting the percentage viability versus concentration on a logarithmic graph and reading off the concentration at which 50% of cells remained viable relative to the control. Each experiment was repeated at least three times to obtain mean values.

2.6.1. Cellular uptake study

A549 cells ($4.0X10^4$ cells $well^{-1}$) plated on cover slips, were incubated with **C1** and alone for different time intervals from 1 to 6 h, fixed with 4% paraformaldehyde for 10 min at room temperature (RT) and washed with PBS. This was followed by treatment with Propidium iodide for 10 min at RT. The cells were washed, mounted in 90% glycerol solution containing Mowiol, an anti-fade reagent, and sealed. Images were acquired using confocal fluorescence microscope (Carl Zeiss, Germany)

2.6.2. AO/EB staining technique (induction of apoptosis)

A549 cells were grown in triplicates *using* a 12 well tissue culture plate and allowed to acclimatize overnight. Next day, cells were treated with **C1-C8** incubated for 12 h. After the incubation, cells were stained with acridine orange and ethidium bromide dyes for 5 min in dark and immediately washed three times with PBS. The cells were then suspended in PBS and photographed on confocal LSM-710 fluorescence microscope.

2.6.3. Nuclear staining

Nuclear staining was performed by reported procedures. Briefly, the cells after exposure with complexes for 12-16 h were washed with PBS and fixed in 3.7% paraformaldehyde for 10 min. The fixed cells were then permeabilized with TBST [50 mM Tris-HCl (pH 7.4), 150 mM NaCl, and 0.1% Triton X-100] for 5 min. Cells were washed with PBS and then DAPI solution (10 μgmL^{-1} in PBS) was added and kept for 5 min. After several washings with PBS, the cells were observed under a fluorescence microscope (Leica DM IL microscope with integrated Leica DFC 320 R2 camera and IL50 image software)

2.6.4. FACScan analysis

A549 cells ($5x10^6$ cells/ml) plated overnight were treated with different concentrations of C1-C8 in DMEM. The cells were then cultured overnight, harvested and fixed using chilled 70% ethanol. The cells were then treated with 50mg/ml RNase A for 6 h at 37 °C, stained with propidium iodide staining solution (20mg/ml PI and in PBS) for 1 h at 4°C and analysed using flow cytometry (FACSCanto, Beckton Dickenson) and the percent cell death as that of the control population was determined.

To determine the pathway of cell death, A549 cells ($1x10^6$ cells/ml) were treated with IC_{50} values of **C1-C8** in DMEM, cells were then cultured for 12 h in complete medium, harvested and washed twice with chilled PBS at 4° C. The cells were re suspended in 100mL annexin-V binding buffer (100 mM HEPES/ NaOH, pH 7.4 containing 140 mM NaCl and 2.5 mM $CaCl_2$) and stained with annexin-V FITC and PI. The cells were gently vortexed and incubated for 15 min at RT in the dark. After incubation, 400mL of binding buffer was added to the cells and analysed immediately using flow cytometry.

3.0 Results and discussions

3.1. Characterization

3.1.1. Mass spectrometry

The ESI-MS spectra of the complexes of the ligands **L1-L8** and complexes **C1–C8** showed molecular ion peaks at m/z values equivalent to their molecular weights. The m/z values of all the complexes are in well agreement with the proposed composition (Fig S3).

3.1.2. FTIR Spectroscopy

The FTIR spectra of the complexes **C1–C8** displayed characteristic strong stretching bands at 1518–1582 cm^{-1} and weaker bands at 1490–1514 cm^{-1} due to asymmetric and symmetric carboxylate (COO^-) stretches respectively, which were found as strong bands in the fingerprint region at 1580–1612 cm^{-1} in the spectra of free mannich bases (L1-L8). The distinct broad bands at ~3450 cm^{-1} owing to the O-H stretching of free carboxylic acid groups found in the ligands are completely lost in the IR spectra of the complexes indicating complexation of the ligands with Cu(II) via the carboxylate oxygen. Furthermore the medium secondary amine N-H stretching bands in the region of 2921–2963 cm^{-1} observed in the spectra of the free ligands, shifted to 2920–2930 cm^{-1} in the complexes indicating complexation via the nitrogen of secondary amine. Similarly the shifts in the pyridone carbonyl $\nu(CO)_{MFL}$ and the carboxylate $\nu(COO)_{MFL}$ stretching frequencies of moxifloxacin in complexes indicate the binding of these groups with the metal ion. All the important stretching values have been tabulated in Table S1.

3.1.3. Electronic Spectra

The electronic absorption spectra of **C1-C8** in DMSO solution were recorded in the region 200-900nm. The electronic spectra of ferrocenyl ligands displayed intense absorption bands in the UV region ascribed to π-π^* intra ligand transition of the cyclopentadienyl rings of ferrocene [40], which were observed to be blue shifted in the spectra of the complexes **C1-C4** (Table 1).

Additional intra ligand transition bands corresponding to the MFL ligands were observed at 290nm and between 335-340 nm for **C1-C8** slightly shifted to longer wave length due to coordination with Cu (II). All the complexes showed peaks in the region 400-420nm corresponding to MLCT transitions and broad absorptions in the range 620-640 nm (Fig.S4) attributed to d–d transitions for Cu (II) in square pyramidal geometry [41].

The ESR spectra of **C2** (Fig.1) and **C7** were recorded in DMSO at 10 K using 90 KHz field modulation and the *g* factors were quoted relative to the standard marker TCNE (g = 2.00277). The EPR spectra of the complexes exhibit a good hyperfine splitting (Fig.1) and the corresponding $g_{\|}$, $g\perp$ and $A_{\|}$ values are tabulated in Table 2. The values ($g_{II} > g_{\perp} > 2.0023$) for the complexes indicate that the unpaired electron of Cu (II) most likely resides in d_{x2-y2} orbital having $^2B_{1g}$ as ground state and the complexes have distorted square pyramidal geometry [42]. The axial symmetry parameter (G>4) indicates that there are no spin exchange interactions between the copper centres.

Table 1: Electronic spectral data of complexes **C1-C8.**

Compound	Intraligand charge transfer transitions π-π^*	CT Nm	d-d Transition nm
C1	205, 289, 339	406	628
C2	206, 290, 337	417	631
C3	205, 290, 338	402	619
C4	204, 290, 336	409	627
C5	216, 290, 338	402	629
C6	205, 289, 337	402	630
C7	206, 289, 339	402	637
C8	204, 290, 338	402	632

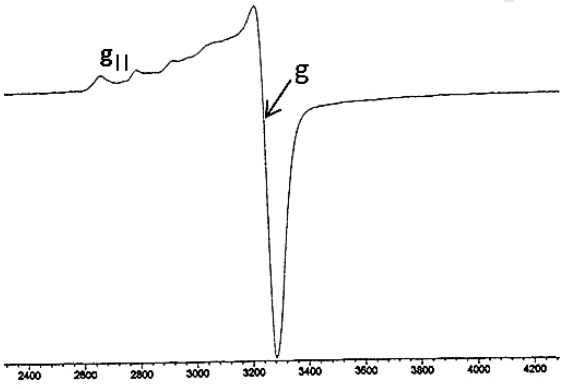

Fig 1: ESR Spectra of **C2** in DMSO.
EPR conditions: Temperature, 10K; microwave power, 5.0 mW; Modulation amplitude, 1G; microwave frequency, 9.1GHz.

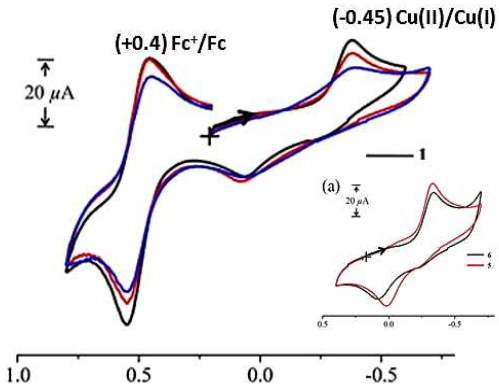

Fig 2: Cyclic voltammogram of **C2** in DMSO. 0.1 M TEAP at a scan speed of 50 mV s^{-1}.
Inset: Cyclic voltammogram of **C5** in DMSO -0.1 M TEAP at a scan speed of 50 mV s^{-1}.

Table 2: ESR and cyclic voltammetry data of complexes **C1-C8**.

Compounds	C1	C2	C3	C4	C5	C6	C7	C8
$g_{\|\|}$	-	2.23	-	-	-	-	2.32	-
$g_{\perp}$	-	2.09	-	-	-	-	2.12	-
$A_{\|\|}$ (cm^{-1})	-	140×10^{-4}	-	-	-	-	146×10^{-4}	-
$A_{\perp}$ (cm^{-1})	-	48×10^{-4}	-	-	-	-	50×10^{-4}	-
G		4.8					4.2	
Cu^{2+}/Cu^{1+}(mV)	-450	-470	-440	-420	-380	-410	-400	-385
Cu^{1+}/Cu^{2+}(mV)	-290	-290	-285	-250	-250	-255	-250	-245
ΔEp (mV)	-160	-180	-165	-170	-130	-155	-150	-140
Fc^{+}/Fc (mV)	480	470	485	480	-	-	-	-

Complexes **C1-C4** were redox active and displayed a quasi-reversible cyclic voltammetric response near 480 mV vs SCE in DMSO 0.1 M TEAP assignable to the Fc^{+}-Fc couple, where Fc is the ferrocenyl moiety (Fig.2). There is a significant positive shift of~50 mV in the Fe (III)/Fe (II) potential in these complexes compared to that of only ferrocene (430mV vs SCE). The complexes also showed a quasi-reversible cyclic voltammetric response in the range -380 to -470 mV assigned to the Cu (II)/Cu (I) reduction and Cu(I)/Cu(II) oxidation in the -250 to -290mV range (Table 2).

Thermal stability and thermal behaviours of all complexes were studied by thermogravimetric analysis in the temperature range 50–850 $^{\circ}$C in N_2 atmosphere. The thermal behaviour studies of the complexes were found to be similar. The TGA profiles over the temperature range 30–250 $^{\circ}$C are usually due to loss of moisture, water of hydration and coordinated water. The complexes have first decomposition stage in the range 200–250 $^{\circ}$C. This dehydration process probably is due to the loss of coordinated water. Above 250 $^{\circ}$C, complexes decompose in a gradual manner, which may be due to thermal degradation of the organic ligands. The continuous loss of weights is observed up to 700 $^{\circ}$C, leaving CuO as residue (Fig. S5).

3.1 DNA binding studies

3.1.1 UV-Visible absorption titration

The presence of ground state interactions between the biological macromolecule DNA and complexes under study have been detected using absorption spectroscopy. DNA can provide three distinctive binding sites (groove binding outside of DNA helix along major or minor groove, electrostatic binding to phosphate group and intercalation), a behaviour important for the biological role of antibiotic and anticancer drugs in vivo [43]. The binding efficiency of the metal complexes to DNA can be effectively investigated employing electronic spectroscopy since the observed changes in the spectra may give evidence of the existing interaction mode [44]. Any interaction between **C1**–**C8** and DNA is expected to perturb the ligand centred transitions of the compounds.

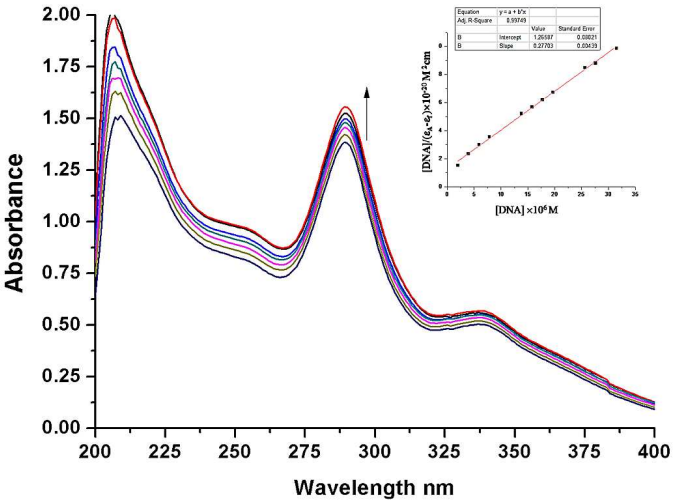

Fig 3: Absorption spectra of **C1** showing the increase in absorption intensity on gradual addition of CT-DNA in 5 mM TrisHCl buffer (pH,7.2) at 25°C. Inset shows the plot of [DNA]/(ε_A-ε_f) vs [DNA].

Binding with DNA via non-intercalative binding modes, such as electrostatic forces, van der Waals interactions, hydrogen bonds and hydrophobic interactions generally results in increase in absorption intensity (hyperchromism) and blue shift of the absorption bands upon increasing the concentration of CT-DNA owing to the degradation of the DNA double helix structure. A blue shift may also be attributed to improper coupling of π* orbital of the ligand and π orbital of the base pairs. This unstacking of base pairs (distortion in π orbital of base pairs and π* orbital of ligand) causes slight blue shift (hypsochromic shift). Similarly reduction of face to face base stacking (exposed electrons) induces enhancement of absorption intensity (hyperchromism). On the other hand intercalation generally results in hypochromism and a red shift (bathochromism) of the absorption band due to a strong stacking interaction between an aromatic moiety of the ligand and the base pairs of the DNA. A red shift can be directly linked with coupling of π* orbital of intercalated compounds with the π orbital of DNA base pairs, thus decreasing π-π* transition

energy. On the other hand the coupling π orbital is partially filled by electrons thus decreasing transition probabilities and concomitantly resulting in hypochromism [45].

The UV spectra of the complexes **C1-C8** (10^{-6} M), have been recorded in the absence and presence of varying CT-DNA concentration (1–50 x 10^{-3} M) within. The bands centred around 289–290 nm and 337-339 nm in the complexes showed significant hyperchromism with red shift (Fig.5 representative data for **C1**), speculative of primarily groove binding nature of the complexes. It should be noted that the exact mode of interaction with DNA cannot be concluded only by UV spectroscopic studies and more techniques should be combined in order to come to a safe conclusion. The results from the UV titration experiments suggest that all complexes can bind to CT DNA [46]; in the cases where an hyperchromic effect exists, a first evidence of binding to CT DNA probably by groove binding may be suggested, while the existence of a red-shift is a hint of a stabilization of the DNA duplex provoked by such interaction [47].

Table 3: DNA binding constants (K_b) of ligands **L1-L8** and complexes **C1-C8**

Compound	% Hypo/Hyper chromism	K_b
L1	18%	6.7×10^4
L2	12%	1.4×10^4
L3	19%	1.3×10^4
L4	20%	5.8×10^4
L5	15%	2.0×10^4
L6	20%	1.5×10^4
L7	17%	4.0×10^4
L8	19%	3.4×10^4
C1	36%	7.0×10^6
C2	25%	2.3×10^6
C3	30%	4.2×10^6
C4	34%	6.4×10^6
C5	39%	6.0×10^5
C6	34%	2.5×10^5
C7	30%	3.4×10^5
C8	36%	5.2×10^5

The magnitude of binding strength to CT-DNA may be determined through the calculation of binding constant K_b which is obtained by monitoring the changes in the absorbance of the compounds with increasing concentrations of CT-DNA. K_b is given by the ratio of slope to the y intercept in plots [DNA]/(εa− εf) versus [DNA]. where $\varepsilon_a = A_{obsd}/$ [compound], ε_f is the extinction coefficient for the unbound ligands and complexes, and ϵ_b is the extinction coefficient for the compounds in the fully bound form. The K_b values of metal complexes showed 10–100 folds higher binding efficacy compared to the ligands. In general, complexes **C1–C4** exhibit stronger binding interactions(10^6 M^{-1}) than complexes **C5–C8** (10^5 M^{-1}) due to strong groove binding of the ferrocenyl moiety (Table 3). Complexes **C1** and **C4** with tryptophan and tyrosine substituted ferrocenyl moieties bound to the Cu (II) centre respectively show the higher binding constant values due to additional hydrogen bonding interactions between the NH group of

tryptophan and the –OH group of tyrosine with DNA nucleobases which are accessible both in major groove and minor groove.

3.1.2 Fluorescence quenching Studies

To further examine the mode of interaction of the compounds with DNA, via intercalation or groove binding, a competitive binding study with two dyes: EB and DAPI have been carried out using steady state fluorescence spectroscopy. Ethidium bromide (=3,8-diamino-5-ethyl-6-phenyl-phenanthridinium bromide) is a phenanthridine fluorescence dye and is a typical indicator of intercalation, forming soluble complexes with nucleic acids and emitting intense fluorescence in the presence of CT DNA due to the intercalation of the planar phenanthridinium ring between adjacent base pairs on the double helix [48]. Addition of a second molecule, which may replace EB and bind to DNA via intercalation results in a decrease of the DNA-induced EB emission [49]. The emission spectra of DNA–EB (λ_{ex}= 546 nm, λ_{em}= 610) in the absence and presence of increasing amounts of ligands and complexes have been recorded. Addition of the complexes **C1–C8** did not have any kind of effect on the emission intensity or nature of the emission of DNA–EB complex, indicating that intercalation may not be the binding mode for these compounds.

3.1.3 Competitive binding studies with DAPI

DAPI (4,6-diamidino-2-phenylindole) is a classical minor groove binder to DNA and binds specifically to GC regions. The fluorescence of DAPI (5µM) increases approximately 30 times when 20-fold excess (base pairs) of DNA (20µM) is added to the solution of the dye [50,51]. The fluorescence spectra of a mixture of DNA–DAPI solution with increasing concentration of **C1–C8** (0-100µM) have been recorded . The addition of aliquots of the complexes cause an initial fluorescence enhancement (Fig.4, red lines) which on further addition of greater amounts showed subsequent quenching of the DNA–DAPI fluorescence (Fig.4, blue lines). The initial fluorescence enhancement can be attributed to partial overlap of the electronic states of the quencher molecules (**C1–C8**) and DNA–DAPI complex leading to partial stabilization of the ground state complex and an increase in the value of the Franck–Condon factor. The fluorescence intensity is

proportional to the overlap of vibrational wave functions and consequently to the Franck–Condon factor.

A quencher molecule when approaches a DNA–DAPI complex, forms an intermediate complex, which is temporarily more stable than the original DNA– DAPI complex. This shifts the ground electronic state to left and down, and as a result the overlap between the vibrational functions in the excited and ground electronic states increases due to the Frank–Condon principle (greater the overlap between the vibrational functions of excited and ground states of the complex, greater is the Franck–Condon factor), leading to the increase in fluorescence signal. Further addition of the quencher leads to the complete displacement of DAPI from the DNA helix and fluorescence depletion [21, 52]. This phenomenon has been explained schematically in Fig.4. The quenching of the DNA–DAPI fluorescence is conclusive of the fact that **C1–C8** replace DAPI from the minor grooves of DNA and get bound, indicating their preference for groove binding.

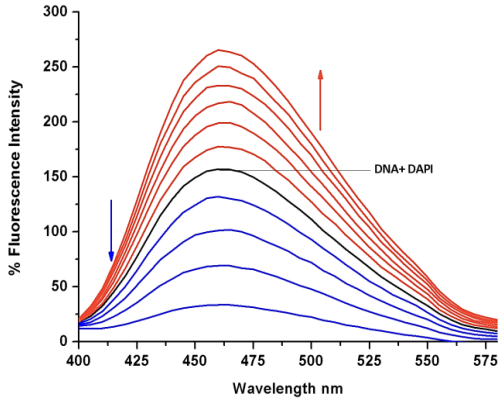

Fig 4: Emission titration of DNA-Dapi complex with increasing concentration of **C1**.
Red lines = changes in 1st phase (increasing intensity); blue lines= changes in 2nd phase (decreasing intensity).

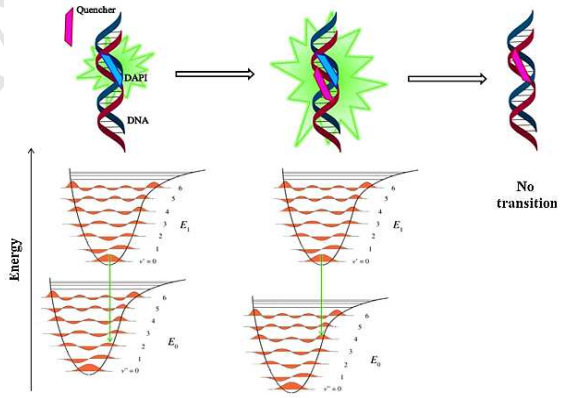

Fig 4: Schematic presentation of DAPI displacement from DNA helix by quencher molecule followed by fluorescence quenching and corresponding energy diagrams.

3.1.4 Viscosity Measurement

In order to further confirm the mode of binding of complexes **C1–C8** to CT-DNA, viscosity measurements of DNA solutions were carried out in presence and absence of these complexes. The viscosity of DNA is sensitive to length changes and is regarded as the least ambiguous and the most critical clues of a DNA binding mode in solution [53]. In general, intercalating agents are expected to elongate the double helix to accommodate the ligands in between the base pairs, leading to an increase in the viscosity of DNA. In

contrast, a complex that binds exclusively in the DNA grooves typically causes less pronounced (positive or negative) or no changes in DNA solution viscosity [54].

The effects of the complexes **C1–C8,** the classical intercalator EB and the groove binder dapi on the viscosities of CT-DNA solution are shown in Fig. 5. with increasing [complex] / [DNA] concentration ratios no significant change in the relative viscosity of CT-DNA solution was observed which ruled out intercalative binding mode of complexes and is consistent with the DNA groove binding as indicated by DNA–DAPI competitive binding studies.

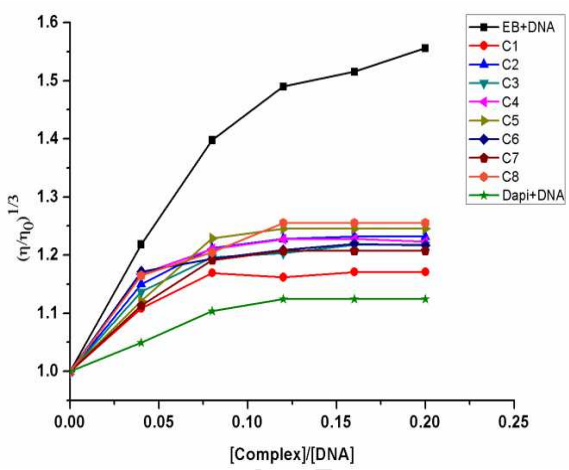

.

Fig 5 : Effect of increasing amounts of the complexes **C1 C8**, dapi and ethidium bromide(EB) on the relative viscosity of CT-DNA (200 mM) in Tris–HCl buffer at 25 ^{o}C [Complex]/[DNA] = 0,0.04, 0.08, 0.12,0.16, 0.20

3.1.5 Nuclease activity

In order to explore the DNA cleavage activity of the complexes, pBR322 DNA (30µM) was incubated with **C1-C8** (10µM) in 5mM Tris–HCl / 50mM NaCl buffer solution (pH 7.2).The DNA cleavage activity was assessed by the conversion of supercoiled form of DNA (Form I, SC) to linear open circular DNA (Form II, OC) or nicked circular (Form III, NC). It was found that all the complexes exhibited DNA cleavage by the conversion of SC Form (I) into OC Form (II) (Fig. 6), which indicates that the complexes are involved in the cleavage through single strand breaking. The control experiments with the ligands or $CuCl_2 \cdot 2H_2O$ or DNA alone do not reveal any significant cleavage, As the complexes do not require an external agent like

ascorbic acid, MPA, or H_2O_2 for cleavage, it is evident that DNA cleavage occurs via an oxidative pathway only.

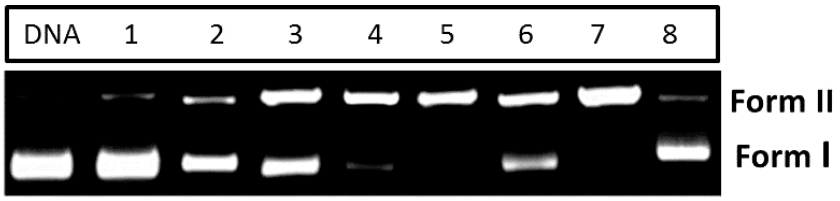

Fig 6: Photogenic view of interaction of pBR322 DNA (30 µg/mL) with 10 µM complexes incubated for 2hours at 37 °C: Lane 1, **DNA**; Lane 2, DNA+**C1**; Lane 3, DNA + **C2**; Lane 4, DNA + **C3**; Lane 5, DNA + **C4**; Lane 6, DNA + **C5**; Lane 7, DNA +**C6**; Lane 8, DNA +**C8**.

4.0 Cytotoxicity studies

4.1 MTT assay

3-(4,5-Dimethylthiazol-2-yl)-2,5-diphenyltetrazolium bromide (MTT) assay was done to test the ability of compounds to inhibit cell growth and induce cell death in A549 cells (human lung carcinoma). A549 cells were treated with the compounds at varying concentrations (15–250µg/ml) for 12 h which inhibited the growth of A549 lung cancer cells significantly in a dose and time dependent manner and the complexes recorded 50–85% higher cytotoxicity compared to the ligands. The IC_{50} values shown in Fig.7 indicate the order of cytotoxicity as **C7** < **C6** < **C8** < **C5** < **C3** < **C2** < **C4** <**C1**.The results reveal enhancement in the antiproliferative activity of the parent fluoroquinolone ligand (MFL) upon metal ion(Cu^{2+}) conjugation giving credence to the hypothesis that biological activity of such fluoroquinolones may partly be related to their metal

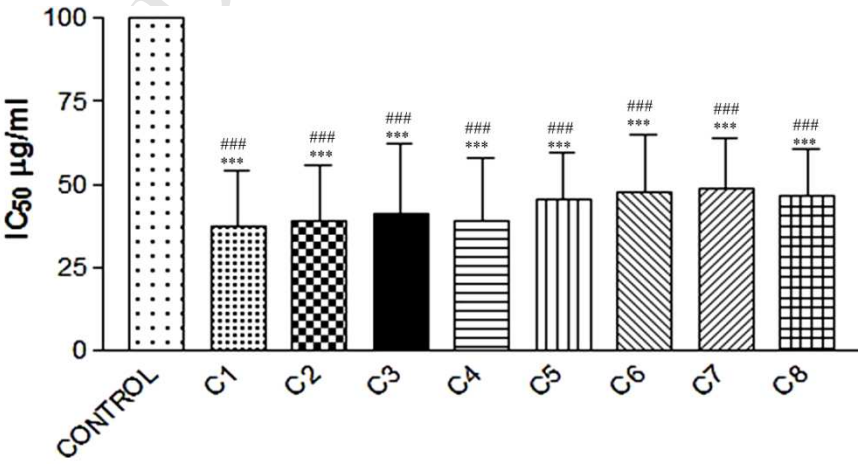

Fig.7: MTT data expressed as mean ±S.E.M. for n=3. Where, ***p<0.001 compared to Ligands (**L1-L8**) and ###p<0.001 compared to MFL. 50% inhibition concentration (IC_{50}µg/ml) for complexes **C1–C8**.

chelating ability. Cell viability assay using control compounds showed that the ligands and the metal salt alone were nontoxic to the cancer cells. Amongst the compounds examined presently, **C1** seems to be the most potent molecule.

4.3 Cellular uptake study

The cellular uptake and localization of **C1-C8**, was studied by using confocal microscopy [55]. A549 cells were cultured on coverslips (corning22x22 mm), incubated for 24 h until they reached 70% confluency. These were then serum starved overnight, followed by incubation with **C1-C8** (IC_{50}), for 6h at 37 °C. Confocal microscopy imaging was carried out by staining with PI (nuclear stain) to identify localization of the complexes and any nuclear disintegration. After treatment for 6 h, bright blue fluorescence in the cytoplasm of the cells was observed under confocal microscope (Fig. 8A), indicating the uptake of complexes by cells. Fig.8B shows uptake of PI by nucleus only and Fig. 8C is merged image of Fig.8A and B, which confirms the uptake and accumulation of complexes in cytosol of the cells. Cells not treated with complexes exhibited negligible luminescence. Fluorescence intensity was found to increase with time indicating increased internalization of the complexes. These results indicated that **C1-C8** can enter and accumulate in the cytosol of cells.

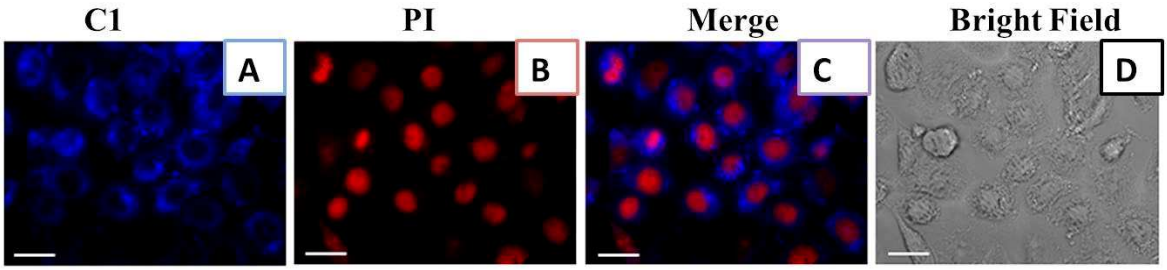

Fig 8: Confocal microscopic images of A549 cells treated with C1 and PI (A) blue emission of C1 (B) nucleus stained with PI (C) Merged image of A and B (D) Bright field image of A549 cells treated with C1 for 6 hr at 37^{o}C.

4.4 Induction of Apoptosis

Apoptosis induced by compounds is one of the considerations in drug development. The apoptotic cells usually show characteristic apoptotic features such as nuclear shrinkage and chromatin condensation. Apoptosis assay was carried out with staining methods using acridine orange (AO) and ethidium bromide (EB). The AO/EB staining is sensitive to DNA and was used to assess the changes in nuclear morphology. Apoptotic and necrotic cells can be distinguished from one another using fluorescence microscopy. In the absence of **C1**, the living cells were stained bright green (Fig. 9, control). After treatment of A549 cell line with **C1** for a period of 12 h, green apoptotic cells containing apoptotic bodies, stained by acridine orange as well as

ethidium bromide were found in addition to red necrotic cells stained by ethidium bromide (Fig. 9). Similar results were observed for all the complexes.

Furthermore, to determine the nuclear features and to gain insight into the pathway of cell death, DAPI staining was carried out in the presence of **C1-C8**. The control cells exhibit light and evenly stained contours of the nuclei in contrast to the treated cells that show typical characteristics of cells undergoing apoptosis. The treated cells are seen to possess fragmented or highly condensed nuclei while the bright field images provide evidence for cell shrinkage and membrane blebbing attributed to the typical features of apoptotic cells (Fig. 9). Necrotic nuclei are not observed with DAPI staining. The DAPI staining indicates apoptotic mode of cell death in the presence of **C1**.Similar results were observed with all the other complexes.

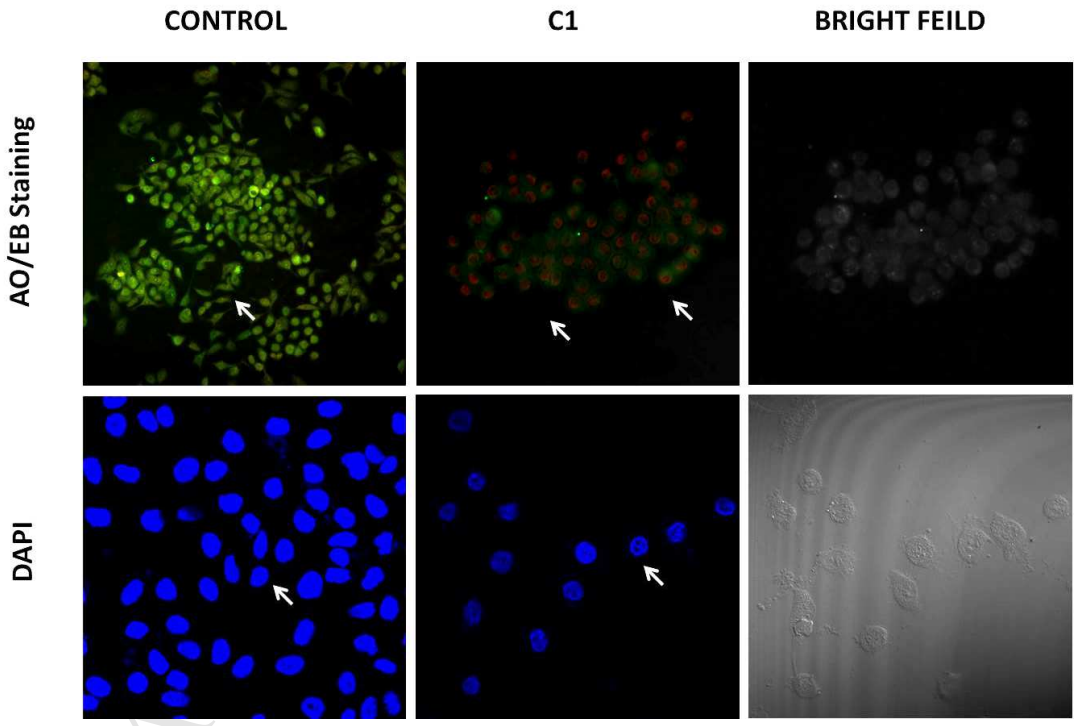

Fig 9: Confocal images of A549 cells treated with **C1** for 12 hr at 37^{o}C in 5% CO_2.
A) Staining with acridine orange/ ethidium bromide. B) Staining with DAPI.

4.5 Cell cycle arrest by flow cytometry

The effect of **C1-C8** on the cell cycle of A 549 cells was studied by flow cytometry in propidium iodide (PI) stained cells after treatment with complexes for 12 h. The representative DNA distribution histograms of control and A549 cells in the presence of **C1**are shown in Fig.10.

Cells go through the cell cycle in several well-controlled phases [56]. The entry into each phase of the cell cycle is carefully regulated by different checkpoints. One of the major focuses of drug discovery is to develop agents that target the cell cycle checkpoints that are responsible for the control of cell cycle phase progression. Cell cycle analysis is used to detect and measure apoptosis, a form of programmed cell death, by analysing cells with less DNA content ("sub-G_1 cells")[56]. Such cells are usually the result of apoptotic DNA fragmentation. Apoptotic cells often have fractional DNA content due to the fact that the fragmented (low MW) DNA undergoes extraction during the staining procedure. Some cells also lose DNA (chromatin) by shedding apoptotic bodies. Thus, only a fraction of the DNA remains within apoptotic cells. Therefore, nuclei of apoptotic cells contain less DNA than nuclei of healthy G_0/G_1 cells, resulting in a sub-G_0/G_1 peak in the fluorescence histogram that can be used to determine the relative amount of apoptotic cells in a sample.

Flow cytometry was used to probe the mode of cell death and cell cycle arrest induced by the complexes, and it was found that after 12 h of incubation the population of G0/G1, S and G2/M cells decreased without significantly affecting the overall cell count (Fig. 10(a)). Moreover, the percentage of DNA content (apoptotic cells) is increased in the Sub G0/G1 phase (Fig.10(a) & (b)) reflecting a significant inhibition of cell cycle progression. Thus, the overall effect of **C1** treatment appears to involve the prevention of cell division followed by cell death with a profile indicative of programmed cell death (apoptosis). Similar results were obtained with complexes **C2-C8** (Fig. 10(b)).

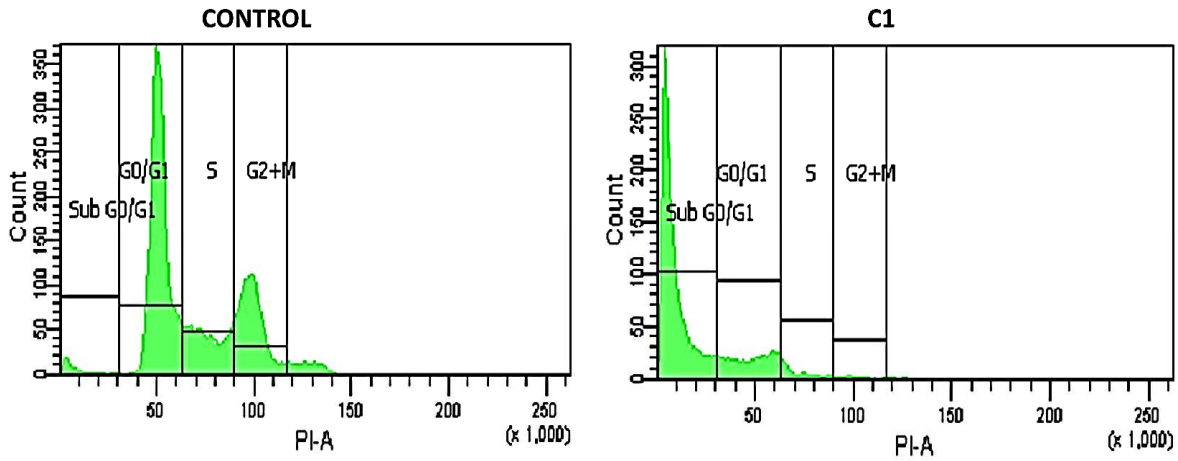

Fig 10 (a): Effects of **C1** on A549 tumour cells after 12 h, distribution among cell cycle phases.

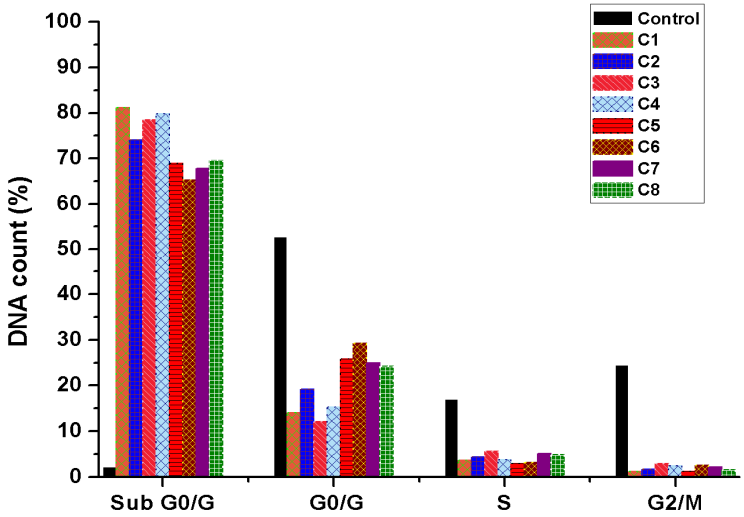

Fig 10 (b): Cell cycle distribution on exposure of A549cells to complexes **C1-C8** (IC_{50}).

An apoptosis study using flow cytometery can be used to distinguish different cell types such as viable cells, early apoptotic cells, and late apoptotic cells [57]. The measurement of annexin V binding to the cell surface as an indicator for apoptosis is performed along with a dye exclusion test to establish the integrity of the cell membrane. Annexin V, a calcium-dependent phospholipid binding protein with high affinity for phosphatidylserine, binds to the phosphatidylserine that has migrated outside the cell membrane. Propidium iodide (PI), a viability stain which binds to the nucleus once the membrane has broken down, is used as an indicator of membrane structural integrity.

A549 cells were incubated with **C1-C8** (IC_{50}) for 12 h, followed by staining with annexin and PI. Data was collected by a flow cytometer. In the early stages of apoptosis, the cell membrane can expose phosphatidylserine, which is annexin V-positive. Viable cells did not bind to annexin V or PI (lower-left quadrant), early apoptotic cells bound to annexin V but excluded PI (lower-right quadrant), and late apoptotic cells were positive for both annexin V and PI (upper-right quadrant). The upper-left quadrant contains dead cells. The results shown in Fig.11 (a) & (b) indicate that the control cells contain 3.59 % late apoptotic cells (upper-right quadrant). The order of the percentage of late apoptotic A549 cells treated with complexes **C1–C8** for 12 h is as follows: **C2** (21.3%) < **C7**(22.8%) < **C5**(27.4%) < **C8** (27.6%) < **C4**(29.3%) < **C6** (31.1%) < **C3**(33.1%) < **C** (36.6 %). Thus it can be concluded that the complexes induce apoptosis in A-549 cells.

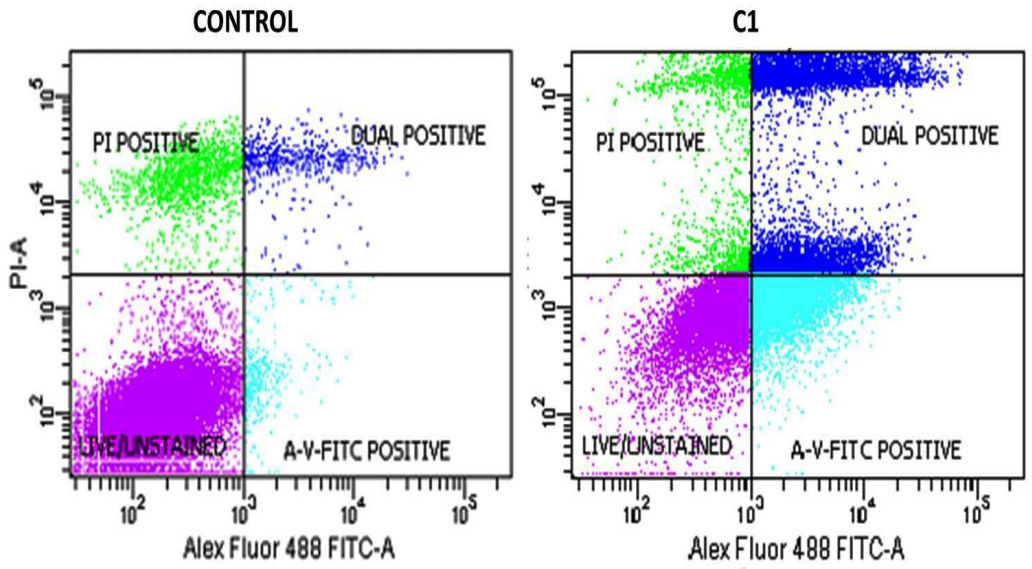

Fig 11 (a): Annexin V staining shows induction of apoptosis of A549 cells treated with **C1** 12 h. The percent of apoptotic cells were detected by analysing Annexin V and PI binding with the help of flow cytometry. Viable cells did not bind to Annexin V or PI (lower left quadrant D3), early apoptotic cells bound to Annexin V but excluded PI (lower right quadrant D4), and late apoptotic cells were both annexin V- and PI-positive (upper right quadrant D2), the upper left quadrant D1 contains the nuclear debris or dead cell.

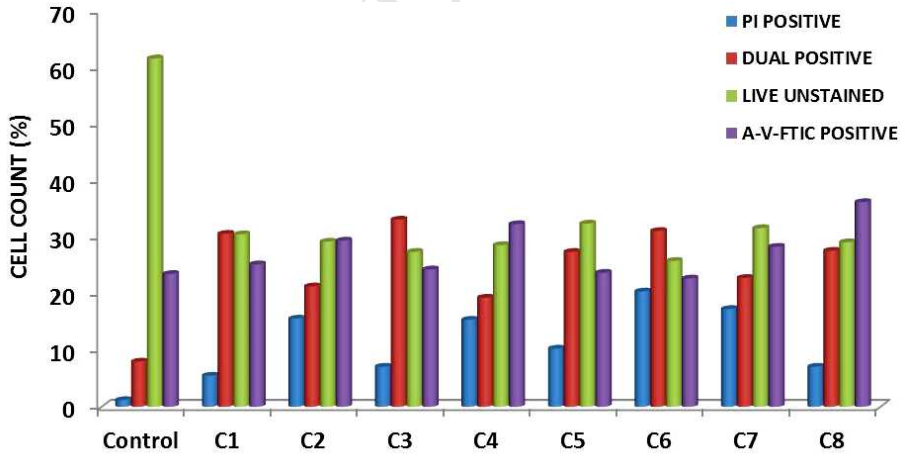

Fig 11(b): Graphical representation of flow-cytometric analysis of apoptosis induced in A549 cells on treatment with **C1-C8** for 12 h. Data is represented in the form of percentage of apoptotic population.

5.0 Conclusion

Ternary Cu (II) complexes with ferrocene and benzene conjugated L-Amino acid mannich bases and the antibiotic drug moxifloxacin were synthesized, characterized and their biological

potential as cytotoxic agents was studied. Binding of these complexes to CT-DNA has been investigated in detail by electronic absorption titration, steady state emission, and viscosity studies. The results suggest that the complexes **C1-C8** are efficient DNA groove binders. The redox active complexes with quasi-reversible Fc^{+} /Fc (**C1-C4**) and Cu(II)/Cu(I) couples display significant chemical nuclease activity (pBR322 DNA) in absence of any external agents. Anti-proliferative effects on A549 tumour cells exerted by the complexes are consistent with their intracellular uptake properties. The cellular uptake indicated that complexes **C1-C8** enter the cytoplasm and accumulate in the nuclei. Rapid change in the nuclear morphology with DAPI staining and acridine orange/ethidium bromide dual staining reveals that most of the A549 cells enter early apoptosis within 12 h of treatment. Further all the complexes show effective cell growth inhibition by triggering G0/G1 phase arrest and inducing apoptosis. FACScan results show remarkably high percentage of cell death induced by the complexes in the A549 cells, as compared to control. Annexin-V/PI staining of cells also indicated that the complexes induce cell death through the apoptotic pathway. Our studies suggest that the complexes are potential anticancer molecules that may interfere with DNA replication. This work makes a significant contribution to the virtually unknown chemistry of organometallic complexes as synthetic nucleases.

Acknowledgement(s)

The authors acknowledge University Grants Commission, New Delhi, India for providing financial support and Department of Science and Technology (DST) for DST INSPIRE Fellowship. Authors are grateful to the Heads, Department of Chemistry and Department of Zoology, The Maharaja Sayajirao University of Baroda, for providing with the necessary laboratory facilities.

References

[1] T. W. Hambley, Dalton Trans., (2007) 4929.

[2] C. Orvig, M. Abrams, J.Chem. Rev., 99 (1999) 2201.

[3] K. H. Thompson, C. Orvig, Dalton Trans., (2006) 761.

[4] F. Arnesano, G. Natile, Coord. Chem. Rev., 253 (2009) 2070.

[5] Y. W. Jung, S. Lippard, J. Chem. Rev., 107 (2007) 1387.

[6] T. Boulikas, A. Pantos, E. Bellis, P. Christofis, Cancer Ther., 5(2007) 537.

[7] S. van Zutphen, J. Reedijk, Coord. Chem. Rev., 249 (2005) 2845.

[8] R. Gust, W. Beck, G. Jaouen, H. Schoenenberger, Coord. Chem. Rev., 253 (2009) 2760.

[9] R. Gust, W. Beck, G. Jaouen, H. Schoenenberger, Coord. Chem. Rev., 253 (2009) 2742.

[10] P. C. A. Bruijnincx, P. J. Sadler, Curr. Opin. Chem. Biol., 12(2008)197.

[11] (a) F. Tisato, C. Marzano, M. Porchia, M. Pellei, C. Santini, Med. Res. Rev., 30 (2010) 708.

(b) G. Jaouen, A. Vessières and S. Top, Chem. Soc. Rev., 44 (2015) 8802.

[12] (a) K. Seio, M. Mizuta, T. Terada, M. Sekine, J. Org. Chem., 70 (2005) 1031.

(b) S. Tardito, L. Marchio, Curr. Med. Chem., 16 (2009) 1325.

[13] (a) R. Gul, M.K. Rauf, A. Badshah, S.S. Azam, M.N. Tahir, A. Khan, Eur. J. Med. Chem., 85 (2014) 438-449.

(b) S. Hussain, A. Badshah, B. Lal, R.A. Hussain, S. Ali, M.N. Tahir, A.A. Altaf, J. Coord. Chem., 67 (2014) 2148-2159.

(c) T.K. Goswami, S. Gadadhar, M. Roy, M. Nethaji, A.A. Karande, A.R. Chakravarty, Organometallics., 31 (2012) 3010-3021.

[14] A.M. Gellett, P.W. Huber, P.J. Higgins, J. Organomet. Chem., 693 (2008) 2959.

[15] P.J. Higgins, A.M. Gellett, Bioorg. Med. Chem. Lett. 19 (2009) 1614.

[16] A. Nguyen, S. Top, A.Vessieres, P. Pigeon, M. Huche, E. A. Hillard, G. Jaouen, J. Organomet. Chem., 692 (2007) 1219.

[17] C. Biot, G. Glorian, L. A. Maciejewski, J. S. Brocard, O. Domarle, G. Blampain, P. Millet, A. J. Georges, H. Abessolo, D. Dive, J.Lebibi, J. Med. Chem., 40 (1997) 3715.

[18] (a) M. F. R. Fouda, M. M. Abd-Elzaher, R.A. Abdelsamaia, A. A. Labib, Appl. Organomet. Chem., 21 (2007) 613.

(b) C. S. Allardyce, A. Dorcier, C. Scolaro, P. Dyson, J. Appl. Organomet. Chem., 19 (2005) 1.

[19] M. Miwa, H. Tamura, Chem. Lett., (1997) 1177.

[20] B. Maity, M. Roy, A. R. Chakravarty, J. Organomet. Chem., 693(2007) 1395.

[21] P. Ramadevi, R. Singh, S. S. Jana, R. V. Devkar, D. Chakraborty, Journal of Photochem. and Photobio. A: Chemistry., 305(2015) 1.

[22]. P. Ramadevi, R. Singh, S. S. Jana, R.V. Devkar, D. Chakraborty, J. Organomet. Chemistry., 833 (2017) 80.

[23] H.-B. Kraatz, N. Metzler-Nolte, Concepts and Models in Bioinorganic Chemistry; Wiley-VCH: Weinheim, Germany, 2006.

[24] S. J. Lippard, J. M. Berg, Principles of Bioinorganic Chemistry; University Science Books: Mill Valley, CA, 1994.

[25] J. J. R. Frausto da Silva, R. J. P. Williams, The Biological Chemistry of the Elements; Clarendon: Oxford, U. K., 1991

[26] M. Valko, H. Morris, M. T. D. Cronin, Curr. Med. Chem., 12 (2005) 1161.

[27] H. Tapiero, D. M. Townsend, K. D. Tew, Biomed. Pharmacother., 57 (2003) 386.

[28] A. Gupte, R. Mumper, J. Cancer Treat. Rev., 35 (2009) 32.

[29] M. Arredondo, T. M. Nunez, Mol. Aspects Med., 26 (2005) 313.

[30] G. Brewer, J. Drug Discovery Today., 10 (2005) 1103.

[31] V. L. Goodman, G. J. Brewer, S. D. Merajver, Endocr.-Relat. Cancer., 11 (2004) 255.

[32] R. A. Festa, D. Thiele, J.Curr. Biol., 21(2011) 877.

[33] G. Crisponi, V. M. Nurchi, D. Fanni, C. Gerosa, S. Nemolato, G. Faa, Coord. Chem. Rev., 254 (2010) 876.

[34] G. Khan, S. Merajver, Expert Opin. Invest. Drugs., 18 (2009) 541.

[35] C. Santini, M. Pellei, V. Gandin, M. Porchia, F. Tisato, and C. Marzano, Chem. Rev., 114 (2014) 815.

[36] Andriole T. (Ed.) (2000), The Quinolones, third ed., Academic Press, San Diego.

[37] R. Singh, R. N. Jadeja, M. C. Thounaojam, R. V. Devkar, D. Chakraborty. Transition Metal Chemistry., 37 (2012) 541.

[38] R. Singh, R. N. Jadeja, M. C. Thounaojam, R. V. Devkar, D. Chakraborty, Inorganic chemistry communications, 23 (2012) 78.

[39] J. Tauchman, G. Süss-Fink, P. Stepnicka, O. Zava, P.J. Dyson, J. Organomet. Chem. 723 (2013) 233.

[40] T. K. Goswami, B. V. S. K. Chakravarthi, M. Roy, A. A. Karande, and A. R. Chakravarty, Inorg. Chem., 50 (2011) 8452.

[41] M. Melnik, Coord. Chem. Rev., 36 (1981) 1.

[42] R. Singh, R.N. Jadeja, M.C. Thounaojam, R.V. Devkar, D. Chakraborty**,** Inorg. chem. comm., 23 (2012) 78.

[43] J. M. Kelly, A.B. Tossi, D.J. McConnell, Nucleic Acids Res., 13 (1985) 6017.

[44] G. Son, J. Yeo, M. Kim, S. Kim, A. Holmen, B. Akerman, B. Norden, J. Am. Chem.Soc., 120 (1998) 6451.

[45] S. Tabassum, W.M. Al–Asbahy, M. Afzal, F. Manalshamsi, Arjmand, J. Lumin., 132 (2012) 3058.

[46] E.S. Koumousi, M. Zampakou, C.P. Raptopoulou, V. Psycharis, C.M. Beavers, S.J. Teat, G. Psomas, T.C. Stamatatos, Inorg. Chem., 51 (2012) 7699.

[47] C. Tolia, A.N. Papadopoulos, C.P. Raptopoulou, V. Psycharis, C. Garino, L. Salassa, G. Psomas, J. Inorg. Biochem., 123 (2013) 53.

[48] S. Dhar, M. Nethaji, A.R. Chakravarty, J. Inorg. Biochem., 99 (2005) 805.

[49] R.F. Pasternack, M. Cacca, B. Keogh, T.A. Stephenson, A.P. Williams, F.J. Gibbs, J. Am. Chem. Soc., 113 (1991) 6835.

[50] S. Eriksson, S.K. Kim, M. Kubista, B. Norden, Biochem., 32 (1993) 2987.

[51] A. Biancardi, T. Biver, F. Secco, B. Mennucci, Phys. Chem., 15 (2013) 4596.

[52] A.K. Williams, S.C. Dasilva, A. Bhatta, B. Rawal, M. Liu, E.A. Korobkova, Anal. Biochem., 422 (2012) 66.

[53] S. Satyanarayana, J.C. Dabrowiak, J.B. Chaires, Biochem., 32 (1993) 2573.

[54] D. Suh, J.B. Chaires, Bioorg. Med. Chem., 3 (1995) 723.

[55] C.J. Sherr, Cancer Res., 60 (2000) 3695.

[56] S.R. Umansky, B.A. Korol, P.A. Nelipovich, Biochim Biophys Acta., 655 (1981) 9.

[57] I. Vermes, C. Haanen, H. Steffens-Nakken, C .J. Reutelingsperger, Immunol Methods., 184 (1995) 39.

Highlights

- Mixed ligand copper complexes of ferrocenyl amino acid mannich bases and Moxifloxacin (MFL) were synthesized and characterized.
- The complexes interact with CT-DNA via groove binding mode.
- Antiproliferative activity of metal complexes on lung carcinoma cells (A549) was investigated.
- The cellular uptake indicated that complexes **C1-C8** enter the cytoplasm and accumulate in the nuclei.
- All the complexes show effective cell growth inhibition by triggering G0/G1 phase arrest and inducing apoptosis.
- FACScan results show remarkably high percentage of cell death induced by the complexes in the A549 cells via apoptotsis.
- Our studies suggest that the complexes are potential anticancer molecules that may interfere with DNA replication.